Fuel 300 (2021) 120985

Contents lists available at ScienceDirect

Fuel

journal homepage: www.elsevier.com/locate/fuel

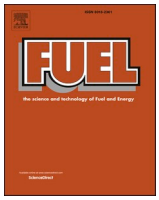

Full Length Article

Scope for biodiesel and bioactive compounds production in the diatom *Nitzschia punctata*

G. Saranya, T.V. Ramachandra *

Indian Institute of Science, Energy & Wetlands Research Group, CES TE 15, New Bioscience Building, Bangalore 560012, India

ARTICLE INFO

Keywords:
Diatoms
Nutritional modes
Mixotrophy
Mucilage (jelly) stalks
Extracellular polymeric substances
Bioactive compounds
Lipids
Biodiesel quality
Eicosapentaenoic acid

ABSTRACT

The isolated diatom *Nitzschia punctata* was subjected to different trophic modes - autotrophy, heterotrophy, and mixotrophy and evaluated variations in growth rate, morphology, biochemical composition, and fatty acid profiles of diatoms in response to different nutritional modes. Glucose was used as a nutrient source in hetero and mixotrophic cultivation. Significant morphological variations in mucilage (jelly) stalks were found in hetero- and mixotrophically grown diatoms. The biomass yield was highest in mixotrophic diatoms (139.16 ± 3 mg/L), followed by autotrophic (127.04 ± 4 mg/L) and heterotrophically grown diatoms (95.22 ± 3 mg/L). Confocal microscopy studies using Nile red revealed significant bright yellow-gold fluorescence dispersed intermittently along with the mucilage stalks of mixotrophic and heterotrophic diatom cultures. Fourier transform infra-red (FTIR) spectroscopic studies showed a sharp absorption peak in hetero- and mixotrophic cultures at 1741 cm-1, indicating the presence of esters of fatty acids (R-C(O)-O-R). Elemental composition analysis using scanning electron microscopy revealed higher C (~48%) in mixotrophic cultivation. Fatty acid methyl esters (FAME) assessment through Gas chromatography and mass spectroscopy (GC–MS) showed higher proportions of palmitoleic acid (C16:1; ~18 – 29%) and oleic acid (C18:1; ~26 – 35%) with saturates and monounsaturates of C16 – C18 up to 90%, confirming of superior biodiesel quality property, which is desirable. The presence of Eicosapentaenoic acid (EPA) in hetero- and mixotrophic cultivation proves the scope for its potential utilisation as a source of bioactive compounds for industrial application.

1. Introduction

Extensive utilisation of fossil fuels has led to negative environmental impacts of global warming and climate change and inducing long-term irreversible effects on human health [1,2], necessitating transition towards renewable energy resources [2,3]. Biodiesel is emerging as a sustainable alternative to conventional fossil fuels due to its renewability and environmentally friendly characteristics [4,5]. The commercial production of biodiesel in India is mainly from animal fats and used cooking oils [6]. However, in recent times microalgae are gaining significant attention and are regarded as promising renewable biofuel resources and value-added bio-products. The composition of microalgae and their growth characteristics are highly influenced by their cultivation conditions [7] as some microalgae are capable of accumulating lipids as high as 50 – 70% under favorable conditions [8]. There are four major types of cultivation: autotrophic, heterotrophic, mixotrophic, and photo-heterotrophic modes [7]. Autotrophic microalgae during photosynthesis transform light energy and inorganic source of carbon (in the form of carbon dioxide) into chemical energies such as polysaccharides, lipids, proteins, and hydrocarbons [9]. The basic requirements of any autotrophic cultures are inorganic carbon sources ($NaHCO_3$), mineral (macro-and micro) nutrients, water, and light [10]. The autotrophic mode has been the most predominant mode of microalgal cultivation [11-14]. Heterotrophic cultivation involves the consumption of exogenous organic carbon substrates through fermentation or aerobic respiration, a mechanism induced especially during the absence of light [15]. Heterotrophic growth involves assimilating organic substrates and subsequent energy generation through aerobic oxygen consumption, termed oxidative phosphorylation [16]. Heterotrophic mode of algal cultivation resulting in increased cell density and productivity is considered cost-effective. It eliminates the requirement of light [17], and growth rates of 0.2 – 0.7 day^{-1} have been reported for many microalgae grown under heterotrophic conditions. The third mode of nutrition is mixotrophy, the mode in which the energy metabolism is harboured through simultaneous respiration and photosynthesis [18], thus requiring both light and organic carbon sources for its growth.

* Corresponding author.
E-mail addresses: tvr@iisc.ac.in, energy.ces@iisc.ac.in (T.V. Ramachandra).

https://doi.org/10.1016/j.fuel.2021.120985
Received 28 March 2020; Received in revised form 27 March 2021; Accepted 2 May 2021
Available online 13 May 2021

Hence, due to the synergetic effects of light and organic substrates, Biomass productivity in mixotrophic mode is the highest among other nutrition modes [19]. Synergism between photosynthesis and organic carbon metabolism in mixotrophic cultivation makes it a potential strategy to achieve higher biomass yield as well as for enhancing the production of target molecules like lipids in microalgal strains [20,21]. Mixotrophic growth modes tend to maximize resource utilisation by eliminating problems associated with limited light availability, thus leading to enhanced growth rate, biomass, and lipid productivity [22]. The maximum specific growth rates in mixotrophic cultivation range between 0.25 and 1.0 day^{-1}. Organic carbon sources widely researched for such heterotrophic and mixotrophic cultivation include glucose, glycerol, and acetate [23]. However, glucose is the most preferred source of carbon substrate in heterotrophic and mixotrophic culture modes [24]. Cultivation of microalgae using glucose as the substrate carbon source among other simple sugars, monohydric alcohols, organic acids, and sugar phosphates showed higher growth rates and respiration [25].

Mixotrophic cultivation mode is considered a successful commercialisation path in microalgae cultivation, especially as a renewable biodiesel feedstock and raw materials for high-value bioproducts (bioactive compounds and food supplements) [17,26]. Diatoms are metabolically flexible organisms with proven characteristics of surviving different growth modes of autotrophy, heterotrophy and mixo-trophy. Diatom species *Amphora* sp., *Navicula saprophila*, *Phaeodactylum tricornutum*, *Cyclotella cryptica*, *Nitzschia* sp. are reported to grow under both heterotrophic and mixotrophic nutrition modes [27]. Higher biomass and lipid productivities were reported earlier in mixotrophic nutrition in microalgae than that of photoautotrophic conditions. Wide variations in fatty acid profiles were reported earlier in diatoms grown under different trophic modes. Also, lipid quality varies significantly with respect to trophic modes, which acts as a major decisive factor of acceptability for its use in biodiesel applications [28]. Diatoms belonging to genera *Navicula*, *Nitzschia* [28,29], *Phaeodactylum* [30-32], and *Cyclotella* [33] grow mixotrophically with varying substrate specificities and assimilation efficiencies [34]. Table 1 presents the diatom strain-wise biomass and lipid productivities as a function of the cultivation and nutrition mode.

The Aquatic Species Program (ASP) [39] provides details on the potential of diatoms to accumulate lipids higher than microalgae and the ability to grow in saline/brackish water [40] and the scope for optimal biodiesel production is being explored [41-43]. In this study, the isolated diatom strain *Nitzschia punctata*. was assessed for its biomass and lipid composition variations under varying nutritional modes. The results revealed significant changes in its growth kinetics and morphological variations with respect to different trophic modes. This variability in lipid content induced through mixotrophy could be of considerable interest in biodiesel production from diatoms.

2. Materials and methods

2.1. Sampling, isolation, and characterisation of diatom isolate

Sediment samples were collected from a salt pan (14°32′39.78″ N, 74°20′59.96″ E) near Uttara Kannada coast in central-western Ghats, India. The top layer of sediments (0.5 cm) was carefully collected by moving a sterile spatula over the moist sediments. The collected sediment samples were serially diluted and subjected to agar plating using artificial seawater, having a salinity of 35 ppt supplementing it with f/2 media composition for its growth. The salt-tolerant marine epipelic diatom *Nitzschia punctata* thus obtained was sequentially scaled up, and pure cultures were maintained with periodic replenishment and subculturing. The concentrated scaled-up diatom culture was subjected to live-cell examination under a high-resolution phase-contrast optical microscope (Olympus BX-51) under 40× magnification and the acid digested [44], processed diatom frustules were visualized under a scanning electron microscope (JEOL – JSM IT 300). The observed live and processed diatoms were digitized (micro-graphed), and the specimen were identified to species level using the standard protocol using morphological identification keys [45,46].

2.2. Microalgae strain and culture conditions

The cultivation was carried out in triplicates in 0.5 L Erlenmeyer flasks by having 0.3 L of culture medium as working volume. Ten days old non-axenic monocultures of *Nitzschia* sp. having a biomass concentration of 0.175 g L^{-1} (dcw) were used as inoculum by adding 10 mL as seed culture volume. Microalgae were cultured at 25 ± 2 °C with a pH of 8.0. Autotrophic cultures were maintained in f/2 media with a light intensity of 60 μE m^{-2} s^{-1} provided by using two LED tube lights

Table 1
Species wise biomass and lipid productivity under different modes of cultivation.

Diatoms	Mode of cultivation	Organic carbon source	Biomass productivity (g L^{-1} d^{-1})	Lipid productivity (g L^{-1} d^{-1})	References
Phaeodactylum tricornutum	Mixotrophy	Glucose	0.053	0.038	[32]
		acetate	0.020	0.017	
		Starch	0.023	0.024	
P. tricornutum	Mixotrophy	Glycerol	*0.713	–	[35]
		acetate	*0.587	–	
		Glucose	*0.555	–	
P. tricornutum UTEX-640	Mixotrophy	Glycerol	0.511	–	[30]
		Fructose	0.379	–	
		Glucose	0.245	–	
Navicula saprophila	Mixotrophy	Sodium acetate	–	+40.5	[28]
Nitzschia sp.	Mixotrophy	Sodium acetate	–	+42.3	[28]
Cylindrotheca fusiformis	Heterotrophy	Lactate, succinate, fumarate and malate	–	–	[36]
Nitzschia angularis	Heterotrophy	Glucose + amino acids	–	–	[29]
Nitzschia laevis UTEX 2047	Heterotrophy	Glucose	*5.5	*0.13	[37]
Cyclotella cryptica	Heterotrophy	glucose	–	–	[33]
Amphora coffeaeformis	Heterotrophy	Glucose	–	–	[38]
		Fructose			
		Glycerol			
		Galactose			
		Acetate			
		Lactate			
		Aspartate			
		Asparagine			
P. tricornutum	Mixotrophy	Soluble fractions of potato	†4.1 × 10^6	–	[31]

*biomass/lipid concentration g L^{-1}; +Lipid content (%) based on dry biomass; †No of cells L^{-1} d^{-1}.

(Philips) having 12:12 h light–dark cycle, while heterotrophic and mixotrophic cultures were maintained in f/2 media along with glucose supplementation of 7.5 g L^{-1} [47]. Dark conditions for heterotrophic cultures were maintained by wrapping the Erlenmeyer flasks with aluminum foil. Appropriate quantities of antibiotics (Chloramphenicol) were added to avoid bacterial contamination during the cultivation period.

2.3. Chlorophyll estimation

Chlorophyll concentration is a surrogate variable used for estimating biomass during cultivation. Chlorophyll estimation was carried out following standard protocols [48]. Aliquots of 10 mL samples were collected on every alternate day from the culture flasks and treated with 1 mL of 1% $MgCO_3$ suspension centrifuged at 7500 rpm in a cooling centrifuge for 10 min at 4 °C. The centrifuged pellets were treated with 8 mL of 90% acetone and stored in darkness for about 20 h with intermittent vigorous shaking. After 20 h, the sample volume was made up to 10 mL, and the contents were centrifuged at 2500 rpm for 5 min. The supernatant was analysed for chlorophyll *a*, c and carotenoids as per Strickland and Parson's equations (1–3).

$$\text{Chl a } (\mu g\ mL^{-1}) = 11.6\ E_{665} - 1.31\ E_{645} - 0.14\ E_{630} \quad (1)$$

$$\text{Chl c } (\mu g\ mL^{-1}) = 55\ E_{630} - 4.64\ E_{665} - 16.3\ E_{645} \quad (2)$$

$$\text{Carotenoids} = 10.0\ E_{480} \quad (3)$$

where E is the absorbance at respective wavelengths.

2.4. Estimation of algal biomass concentration and yield

The stationary phase cultures of the triplicate samples were harvested by centrifugation at 16,500 × g for 10 min at 4 °C in a cooling centrifuge (Beckman Coulter, USA) for biomass yield estimation. The wet algal pellets thus obtained were dried in an oven at 70 °C overnight to obtain dry algal biomass. Biomass concentration based on dry cell weight was determined gravimetrically as per equation (4).

$$\text{Biomass concentration} = \frac{(C_1 - C_0)}{V} (\text{mg L}^{-1}) \quad (4)$$

where C_1 = Final weight of the harvested biomass (mg); C_2 = Initial weight of the algal inoculum (mg); V = volume of the culture media during harvest (L).

Biomass yield was determined by taking the ratio of the algal biomass produced (in heterotrophy and mixotrophy) to that of the amount of glucose consumed during the growth period according to equation (5) (Eqn. (5)).

$$\text{Biomass yield} = \frac{\textit{Weight of the harvested algal biomass (mg)}}{\textit{Amount of glucose utilised (g)}} \quad (5)$$

2.5. Confocal microscopy studies of neutral lipid droplets

In-vivo observation of lipid droplets in live diatom cells was carried out after staining the cells with the Nile red (9-diethylamino-5H- benzo [a] phenoxazine-5-one, Sigma) a fluorescent dye, by preparing the Nile red (NR) solution having a concentration of 0.2 mg/mL in acetone [49]. A known volume (~5 mL) cell suspension from late stationary phase cultures of two timelines (14th and 16th day) was treated with 5 μL of Nile red solution and incubated at 40 °C in dark conditions for 15 min [50]. After incubation, the cells were centrifuged at 7000 rpm for 5 min, washed twice, and re-suspended in autoclaved phosphate-buffered saline (PBS). The NR-stained cells were observed under Zeiss LSM 880 Leica confocal microscope with airy scan having a halogen illuminator for transmitted light with quartz collector with 12 V and 110 W rectangular filament. The laser module of the microscope Argon multiline lasers (458/488/514) and Helium-Neon lasers (543/594/633) nm. The excitation and emission wavelengths were set at 480 nm and 590 – 630 nm [49]. The acquired images were resampled and processed using system-integrated ZEN software.

2.6. Elemental analysis and imaging using SEM-EDS

Elemental analysis and scanning electron microscopic (SEM) imaging of the harvested biomass were carried out in Ultra55 FE-SEM Karl Zeiss (Energy Dispersive X-Ray Spectrometer) EDS, equipped with a fully integrated EsB detector for understanding compositional information. The equipment possesses high-resolution capability with 100 – 900,000× with EsB detector with an acceleration voltage of 0.1 – 30 kV and probe current of 4 pA to 10 nA. The harvested dried biomasses from each nutrition mode were mounted on carbon tapes over an aluminum stub and gold-sputtered before SEM analysis. The field emission images acquired through a high-efficiency In-lens SE detector were analyzed using SmartSEM software.

2.7. ATR FT-IR analysis of algal biomass

The major functional groups of algae were detected using Fourier-transformed infrared (FT-IR) spectroscopy. For infrared analysis, the dried algal biomass was pulverised using a micro pestle and used for ATR GX FTIR (Perkin-Elmer, USA) analysis under transmittance mode between 6000 and 650 cm^{-1} wavelength range. The recorded FT-IR spectra were processed using Spectrum software.

2.8. COD removal efficiency

The glucose utilisation rate or the chemical oxygen demand (COD) removal by heterotrophic and mixotrophic diatom cultures was estimated using DNS (3,5-Dinitrosalicylic Acid) method [51]. A known quantity (~3 mL) of the media supernatant after algal harvest on the 18th day was mixed with DNS reagent A (1% DNS, 0.2% phenol, 0.05% Na_2SO_3, and 1% NaOH) was incubated at 90 °C in a water bath for 5 – 15 min for colour development. Once the reddish-brown colour started to appear, 1 mL reagent B (40% Rochelle's salt) was added to the mixture. The mixture was cooled to room temperature, and the absorbance was recorded at 575 nm in a DR2800 spectrophotometer (HACH, USA). The glucose assimilation efficiency (E) of diatoms was determined using equation 6.

$$\text{COD removal efficiency } E = \frac{[G_0 - G]}{G_0} \times 100 \quad (6)$$

where G_0= glucose concentration in the fresh medium (g); G = residual glucose concentration (g) at the end of the growth period.

2.9. Fatty acid methyl ester (FAME) profiling using GC–MS

Dried algal biomass was subjected to direct transesterification reaction according to [52]. Dried algal biomass (0.1 g) was mixed with 17% H_2SO_4 solution made with 3.4 mL methanol and, a 4.0 mL hexane was additionally added. The direct transesterification reaction was conducted in a DRB 200 heat block by heating the reaction mixture in 10 mL screw-capped glass vials at 90 °C for 40 min with intermittent mixing. After reaction completion, the vials were cooled to room temperature, and 2 mL distilled water was added in order to enable phase separation. The hexane phase containing crude biodiesel (FAME) was recovered, treated with anhydrous sodium sulphate for removing water traces from the organic layer, and analysed for its variation in fatty acid methyl ester FAME profiles with respect to different nutritional modes in an Agilent 7890A GC gas chromatographic system, single quadruple analyzer coupled to an Agilent 5975C inert MSD with triple-axis detector mass Spectroscope with a multimode autosampler. One μL of FAME sample

was injected into the GC system after solubilizing it in hexane (HPLC grade) in split-less mode by using helium as a carrier gas. The flow rate of helium gas was set at 1 mL/min. The mass spectroscope (ms) source and quadruple temperatures were set at 230 °C and 150 °C, respectively. The oven operating conditions was set as 50 °C initially for a hold time of 2 min, then increased at a ramp heating rate of 10 °C/min until 280 °C with a holding time of 4 min. FAME composition was determined in terms of the percentage of total FAMEs present in the sample. The peaks were analysed by comparing the mass spectra with NIST mass spectral database using NIST (2011) integrated with AMDIS software. The mass fractions of each FAMEs were quantified using an enhanced data processing tool. The FAME samples were analysed in triplicates.

2.10. Biodiesel quality testing

Critical biodiesel properties that are required to estimate the quality of biodiesel such as cetane number (CN), iodine value (IV), higher heating value (HHV), specific gravity (SG), kinematic viscosity (KV), and cloud point (CP) were calculated using fatty acid profiles determined through GC–MS analysis. The average degree of unsaturation (ADU) was computed based on mass fraction information of each of the fatty acids derived from fatty acid profiles obtained through GC–MS analysis (Eqn. 7).

$$\mathrm{ADU} = \sum M \times Y_i \tag{7}$$

where M: No of carbon–carbon double bonds in each fatty acid constituent; Y_i: mass fraction of each FA constituent.

Biodiesel properties were determined based on the influence of the degree of unsaturation on biodiesel quality parameters as per equations 8 – 13 [53,54].

$$\mathrm{CN} = -6.6684x + 62.876 \tag{8}$$

$$\mathrm{KV} = -0.6316x + 5.2065 \tag{9}$$

$$\mathrm{CP} = -13.356x + 19.994 \tag{10}$$

$$\mathrm{IV} = 74.373x + 12.71 \tag{11}$$

$$\mathrm{HHV} = 1.7601x + 38.534 \tag{12}$$

$$\mathrm{SG} = -0.0055x + 0.8726 \tag{13}$$

where x = ADU.

3. Results and discussions

3.1. Characteristic features of the diatom isolate

SEM examination of the cultured diatom revealed a clear structural morphology enabling its identification at the species level. The morphological features showed utmost resemblance to the pennate diatom *Nitzschia punctata,* having keel very eccentric, with dots almost always distinct, generally equal in number to those of the striae. Valves are usually sulcate with undulations and rostrate apices [45]. The diatom valve measures ~13. 5 – 14. 5 μm in length and ~5.6 – 6.0 μm in width. The light microscopy and SEM images of *Nitzschia punctata* are given in Fig. 1.

3.2. Morphological variations of the diatom for different nutritional modes

Extracellular polymeric substances (EPS) production is a distinctive characteristic feature of pennate diatoms that form biofilms on the substrate. Diatoms are known to produce copious amounts of mucilage secreted through raphe, which hydrates and swells, thus facilitating adherence of the diatom cells to the substratum [55]. Apart from serving

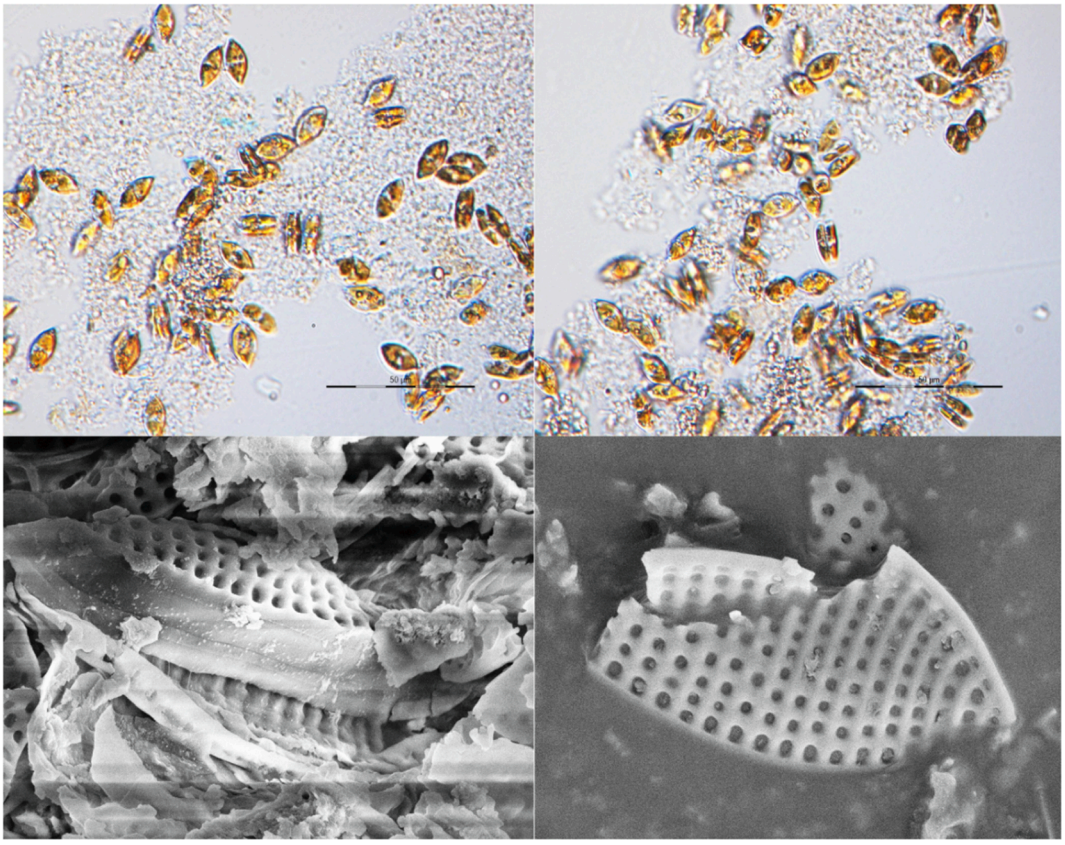

Fig. 1. Light microscopy and SEM images of the diatom *Nitzschia punctata*.

diatoms in locomotion in search of nutrients and available organic sources, these EPS are also responsible for the permanent attachment of sessile microorganisms to sediment particles [56]. Most diatoms exude EPS to colonize, increase cell population, and facilitate biofilm formation through mucilage secretion and subsequent sediment stabilization [57]. Diatoms' exudate extracellular polymeric substances (EPS) of varying compositions. Although polysaccharides are the most abundant component of diatom EPS, heterogeneous mixtures of hexoses, 6-deoxyhexoses, pentoses, N-acetylamino sugars, and O-methylated sugars, and acidic, with uronic acids and/or sulphate esters are present in EPS [58]. EPS secretions can be of diverse morphological forms. Some diatoms produce small pad-like structures at one end of the frustules, whereas some produce fibers, tubes inside which the frustules are enclosed, and some have stalks with nodal attachments of frustules at specific junctions [59]. Characterisation of adhesive mucilage of the diatom *Craspedostauros australis* using atomic force microscopy (AFM) revealed that these are strands secreted from the raphe that are primarily involved in cell-substratum attachment and motility [60]. Earlier studies have reported extracellular mucopolysaccharides to stalk that was exuded from terminal (apical) pore fields in *Cymbella cistula* [59] and *Gomphonema olivaceum* [61]. In the raphid diatom *Gomphonema olivaceum*, the frustules were attached to the transparent jelly-like stalks in linear striations with stalks exuding from the terminal apical pores of the frustules. Extracellular matrix assembly studies on diatoms *Achnanthes longipes*, *Amphora coffeaeformis*, *Cymbella cistula,* and *Cymbella mexicana* exhibited significant variations in stalk morphologies and adhering mechanisms in each diatom. For instance, diatoms *Achnanthes longipes* and *Amphora coffeaeformis* were categorized as capsule producers where the cells have adhered via an organic sheath, and a mucilaginous capsule loosely bounded the cells. In contrast, *Cymbella cistula* and *Cymbella mexicana* were identified as stalk formers where the motile cells were coated by an organic sheath which eventually produces one or two stalks from apical pore fields [62,63]. In the present study, a similar attachment was observed in *Nitzschia punctata* grown in heterotrophic and mixotrophic nutrition modes (Fig. 2) and stalks exuded from the apical pore field.

3.3. Chlorophyll content

Diatoms possess a distinctive pigment composition, unlike other green algae and plants. Only two forms of Chlorophylls, Chl-a and Chl-c, are reported to be present in diatoms apart from carotenoids (a group of photoprotective pigments including β-carotene, diadinoxanthin, and diatoxanthin) [64]. Recent studies have shown that alterations in nutrients (required for algal growth) inducing shifts in metabolic pathways with significant pigment modulations. Thus these pigment alterations are usually considered a proxy for explaining variations in algal growth characteristics as well as fluctuations in its biomass concentrations [47]. Chlorophyll concentrations in this study showed wider variations across different nutritional modes during the growth period. The concentrations of Chl-c were observed to be higher than Chl-a and carotenoids. The maximum concentration of Chl-a (148.3 ± 0.5 μg mL^{-1}) was observed in the autotrophic mode of cultivation, while maximum Chl-c (396.7 ± 7.2 μg mL^{-1}) concentration was observed in mixotrophic cultivation. The maximum chlorophylls concentrations (Chl-a and Chl-c) were reached on the 14th day of operation for phototrophic cultivation and on the 16th day for hetero- and mixotrophic modes of cultivation. Carotenoid's concentration spiked after the 14th day in all three nutritional modes, which could be considered as an onset of stationary phase in the growth period, while Chl-a considerably reduced during the stationary phase. Similar results were observed earlier, in marine diatoms *Chaetoceros* sp., *Skeletonema* sp. and *Thalassiosira* sp. with almost 50% reduction in Chl-a during the stationary phase with a corresponding increase in carotenoid pigments [64,65].

Moreover, nutrient exhaustion triggers the stress phase in algal cells with subsequent chlorophyll, especially Chl-a degradation into simpler compounds [47]. The pigment concentrations (Chl-a, Chl-c, and carotenoids) underwent an initial lag phase in heterotrophic and mixotrophic cultures, whereas the autotrophic cultures exhibited a steady exponential (log) phase right from inoculation till the stationary phase. Carotenoid pigments were the highest for phototrophic cultures, followed by mixotrophic and heterotrophic cultures. Heterotrophic cultures exhibited the most negligible concentrations of chlorophylls and carotenoids. Yet, a gradual increase in trend was observed throughout the growth period, with significantly higher levels recorded during the stationary phase. An increase in chlorophyll content observed in strict heterotrophic systems could be due to the constitutive expression of the photosystems (PSI and PSII) responsible for carrying out photosynthesis [66]. Fig. 3 illustrates the variations in the levels of Chl-a, Chl-c, and carotenoids in diatoms subjected to different trophic modes during the growth period.

3.4. Estimation of biomass concentration and yield

Maximum biomass concentration was achieved in mixotrophic cultivation of *Nitzschia* sp. with 139.2 ± 3 mg L^{-1} (productivity: 7.3 mg L^{-1} d^{-1}), followed by autotrophy (127.04 ± 4 mg L^{-1}) with biomass productivity of 7.05 mg L^{-1} d^{-1} and heterotrophic mode of cultivation exhibited the least biomass concentration (95.2 ± 3 mg/L, productivity 5.2 mg L^{-1} d^{-1}). Mixotrophic cultivation of *Chlorella sorokiniana,* when supplemented with 7.5 g L^{-1} of glucose, showed the maximum biomass concentration of 3.59 g L^{-1} when compared to other nutritional modes

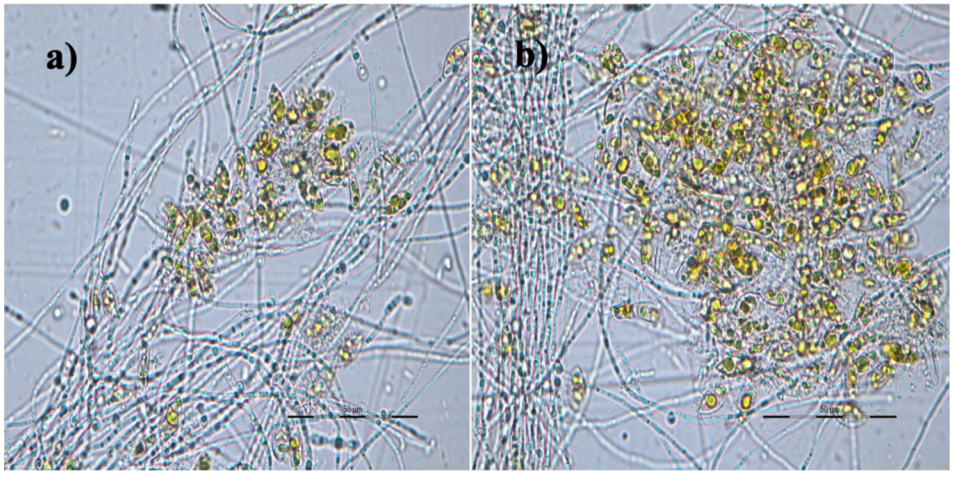

Fig. 2. EPS secretion in the form of mucilage stalks observed in (a) heterotrophic and (b) mixotrophic nutrition modes.

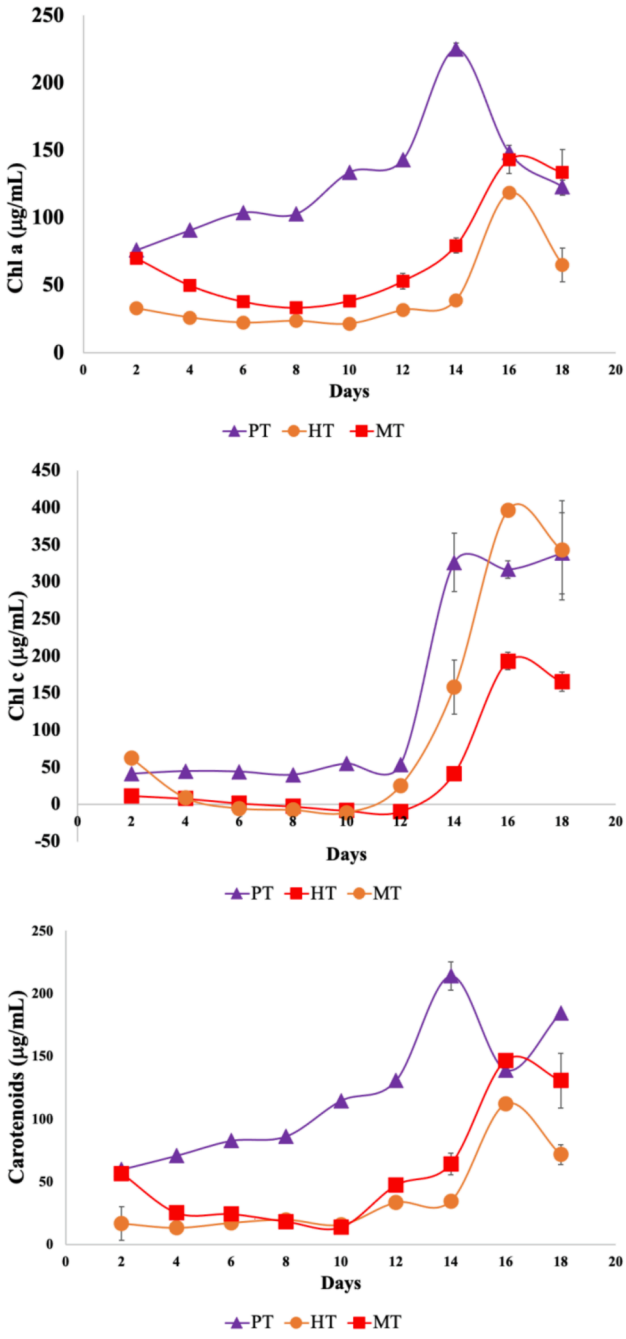

Fig. 3. Variation in chlorophyll a and c (a, b) and carotenoids (c) in different nutritional modes.

[3]. The green microalga *Chlorella vulgaris* showed 4.2 g L^{-1} when 12 g L^{-1} of glucose was used as the organic carbon source [67]. Maximum biomass concentration obtained when *Chlorella* sp. SVMBIOEN3 was cultivated using 7.5 g L^{-1} of glucose under mixotrophic mode was 3.59 g L^{-1} followed by heterotrophic (1.58 g L^{-1}) and autotrophic (0.59 g L^{-1}) [47]. Among diatoms, *Phaeodactylum tricornutum* was reported to exhibit higher biomass concentration (16.2 g L^{-1}) when supplemented with glycerol as an organic carbon source which is estimated to be eightfold more elevated than the autotrophic culture [18]. Mixotrophic assimilation of glucose involves the glycolytic process in the presence of light through the Emden-Meyerhof (EM) pathway [27]. In mixotrophy, both light (photo-phosphorylation) and glucose (oxidative phosphorylation) contribute to ATP production leading to higher energy assimilation, thus leading to higher biomass [68]. The biomass yield calculated by considering the quantity of the biomass produced to that of the amount of substrate (glucose) utilised in hetero- and mixotrophic cultivation yielded 2.54 mg/g and 2.83 mg/g of glucose, respectively. Fig. 4 illustrates the biomass concentration and yield obtained in different trophic modes.

3.5. Nile red fluorescence studies

Nile red is a lipid-soluble fluorescent dye capable of Insitu lipid staining, a method highly beneficial for evaluating lipid content in various mammalian cells and microorganisms such as microalgae, bacteria, and yeast [69]. Nile red staining enables Insitu visualization and quantification of neutral lipid droplets in live algal cells. Confocal microscopy studies on the Nile red-stained diatom strain exhibited conspicuous yellow-gold fluorescence, an indicative factor of neutral lipid accumulation in photoautotrophic cultures (Fig. 5a). In heterotrophic and mixotrophic diatom cultures, peculiar mucilaginous stalks were observed with bright fluorescent lipid droplets uniformly distributed all over the stalks (Fig. 5b-c).

3.6. FE SEM-EDS imaging and elemental analysis

SEM micrographs revealed significant morphological variations in biomass grown under varying trophic modes. Fig. 6 (a-c) presents the morphological variations of the examined microalga grown under autotrophy exhibiting intact structural morphology of natural biomass to that of the treated biomass with organic carbon sources visualized as deformed cell structures in hetero and mixotrophy. Table 2 shows the composition (percent) of elements present in biomass grown under different nutritional modes. SEM-EDS analysis of the harvested diatom biomasses acquired by subjecting diatoms to different nutritional modes revealed a higher organic carbon (C) content of ~48% in mixotrophic (MT), ~35% in heterotrophic (HT), and ~27% in phototrophic (PT) cultivation mode. The higher proportion of carbon in mixotrophic and heterotrophic cultures could be due to excessive extracellular polysaccharides (EPS) secretions in the form of stalks observed in respective culture conditions during microscopic examinations. SEM EDX elemental analysis of *Desmodesmus* sp. grown heterotrophically using sugarcane stillage exhibited higher carbon and oxygen contents of about ~80 – 83% and ~15 – 18%, respectively [70]. The elemental composition of *Chlorella vulgaris* grown autotrophically showed ~51.4 – 72.6% C; ~11.6 – 28.5% O by weight in SEM EDX analysis which is higher when compared to the results of the present study. The elements oxygen (O) and silica (Si) content was observed to be the highest in PT (~47%; ~17%) when compared to MT (~38%; ~ 8%) and HT (~27%; ~4%). Higher silica content (~17%) in the PT cultures could be attributed to rapid multiplication rates under light conditions, while in HT and MT, most of the energy assimilated was routed to EPS secretions and accumulation of energy reserves in the form of neutral lipids. A higher proportion of N was found in HT (~31%), while it was absent in PT and MT. Other minerals like Na, K, Cl, Mg, and S were present in trace amounts (1.03 – 1.99% Na; 0.47 – 1.94% S; 0.48 – 0.56% K; 1.98 – 3.18% Cl; 2.33% Mg) in all the three types of diatom biomasses. Algal biomasses are known to be rich in inorganic mineral nutrients such as calcium, silicon, magnesium, and potassium [70]. *Desmodesmus* sp. exhibited mineral constituents of about 0.07% Na; 0.25% S; 0.09% K; and 0.11% Mg which were comparatively lesser than the levels found in *Nitzschia* sp. in this study [70].

3.7. FTIR analysis

Fig. 7 represents the peaks obtained during FTIR analysis of diatoms grown under different trophic modes. ATR-FTIR spectral analysis of algal samples subjected to different trophic modes showed eight distinct absorption bands (corresponding to wave numbers ranging between 3800 cm^{-1} to 680 cm^{-1}). The infra-red spectrum showing a broad

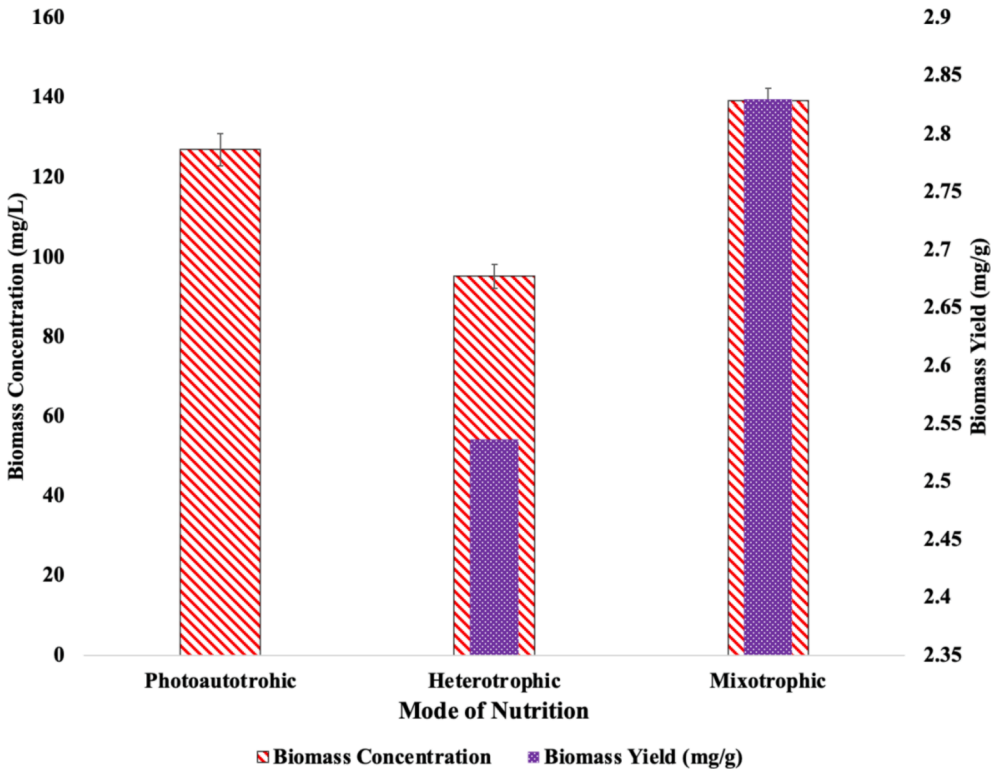

Fig. 4. Biomass concentration and yield w.r.t different modes of nutrition.

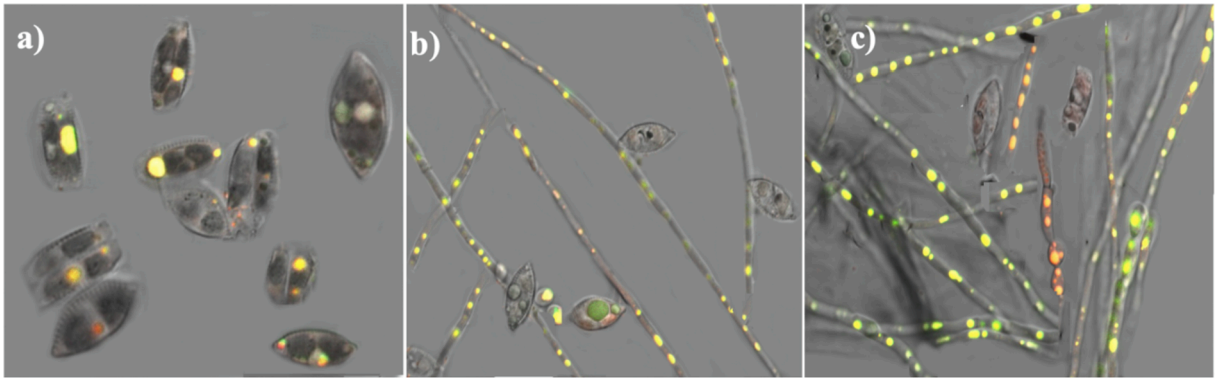

Fig. 5. Confocal images of diatoms showing bright yellow-gold fluorescence of neutral lipids a) autotrophy (PT), b) heterotrophy (HT), and c) mixotrophy (MT). (For interpretation of the references to colour in this figure legend, the reader is referred to the web version of this article.)

absorption peak at 3285 cm^{-1} with a frequency range between 3500 and 3300 cm^{-1} represents N – H Stretching vibration depicting the presence of secondary amines functional group in the form of proteins and lipids. The peak (2923 cm^{-1}) with frequency ranges 2925 – 2875 cm^{-1} represents the aliphatic C – H stretching vibrations of carboxylic (fatty) acids. The presence of sharp absorption at 1741 cm^{-1} (the highlighted portion in Fig. 7) within the frequency ranges from 1750 to 1735 cm^{-1} in both hetero and mixotrophically grown cultures except for phototrophic cultures proved the presence of esters of carboxylic acid (R-C(O)-O-R), especially lipids and fatty acids, a characteristic feature noted in glucose fed diatom cultures. Another strong absorption peak at 1633 cm^{-1} with frequency ranges between 1580 and 1650 cm^{-1} represents the presence of N – H bending vibrations with β carbonyl (unsaturated) ketone amide.

The shoulder peak at 1545 cm^{-1} (1545 – 1542 cm^{-1}) represents C – O vibrations as in – COOR group. The frequency ranges from 1435 to 1405 cm^{-1} with a wide peak at 1455 cm^{-1} represents C–H bending (scissoring) vibrations in CH_3 groups. The frequency ranges 1120 – 1030 cm^{-1} depicts either the presence of symmetric C – H stretching vibrations, especially due to the presence of antioxidant enzymes or γ C-O-C polysaccharides due to the secretion of EPS. The strong peak ranging between 1036 and 1067 cm^{-1} among all trophic mode cultures elucidate the presence of frustule silica (Si-O) tangled over the tubular polysaccharides (as shown in Fig. 2). The weak absorptions at (708 cm^{-1}) with the frequency ranges of 780 – 700 cm^{-1} represent the cis = C – H out-of-plane bending of the aliphatic fatty acids. The FTIR spectra of pure lipid compounds revealed distinct absorption peaks at 3025 – 2954 cm^{-1} of CH_3, CH_2 bonds, and 1746 – 1654 cm^{-1} of C = O ester that are found to be the most characteristic spectrum of lipids, the results of which correlate well with the results of the present study [71]. In an earlier study, the weak bond at 1155 cm^{-1} in the FTIR spectrum of *Cyclotella meneghiniana belongs to C – O vibrations of carbohydrates during photoautotrophy* immediate disappearance of the same during heterotrophy indicates carbohydrates degradation [72]. The absence of a peak

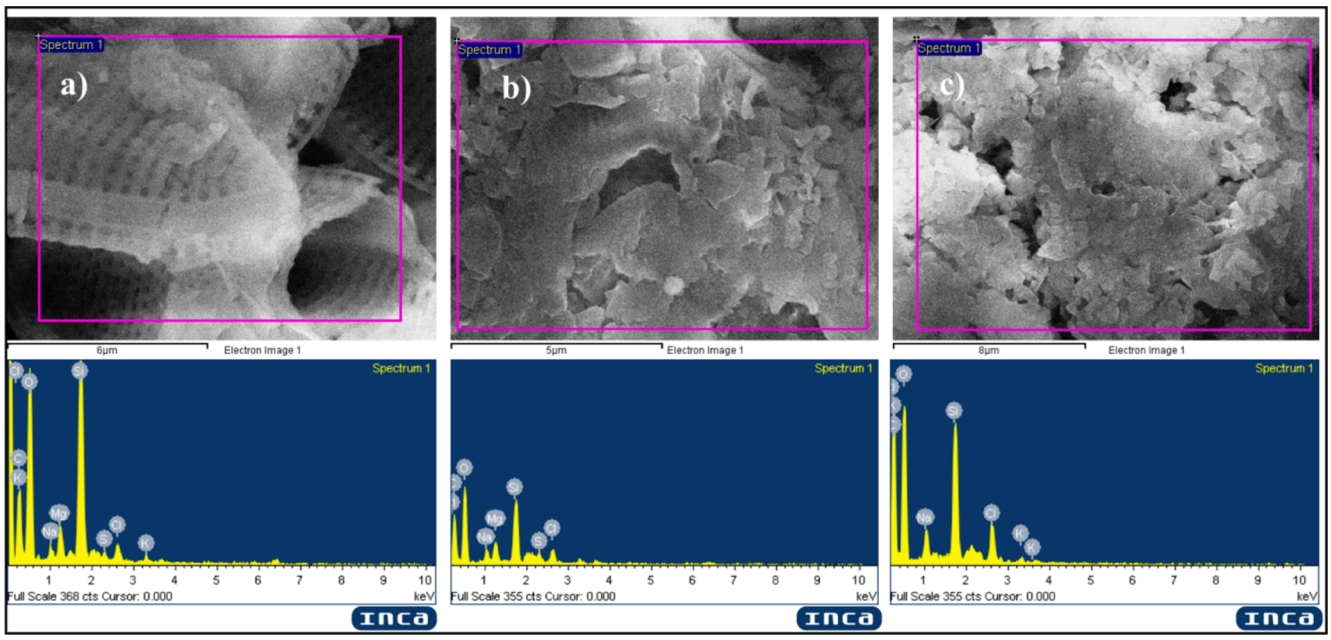

Fig. 6. SEM-EDS showing elemental composition variation across different nutritional modes a) PT, b) HT, and c) MT.

Table 2
SEM-EDS elemental compositions of diatoms under different modes of cultivation.

Element	Photoautotrophic		Heterotrophic		Mixotrophic	
	Weight %	Atomic %	Weight %	Atomic %	Weight %	Atomic %
C K	29.65	39.56	35.41	41.59	47.97	58.19
N K	–	–	31.30	31.52	–	–
O K	47.14	47.22	27.11	23.90	38.27	34.85
Na K	1.03	0.72	–	–	1.99	1.26
Mg K	2.33	1.54	–	–	–	–
Si K	16.85	9.61	4.24	2.13	8.11	4.21
S K	0.47	0.24	1.94	0.86	–	–
Cl K	1.98	0.89	–	–	3.18	1.31
K K	0.56	0.23	–	–	0.48	0.18
Total	100	100			100	

at 1155 cm^{-1} in the present study infers similar results of the absence of complex carbohydrates.

3.8. COD removal efficiency

The initial glucose concentration of 7.5 g L^{-1} COD was reduced to 4.7 g L^{-1} COD with a removal efficiency of ~38% in heterotrophic mode, whereas in mixotrophic mode, the COD removal efficiency was ~50% with a final glucose concentration of 3.7 g L^{-1} (Fig. 8). The rate of glucose utilisation of the present study reveals only 50% COD removal by the diatoms for its EPS production in mucilage stalks in hetero- and mixotrophic cultivation, whereas the remaining glucose was left unutilised. Optimisation of the substrate (glucose) in future studies would bring down the quantity of substrates used for achieving maximum biomass concentration.

3.9. FAME compositional profiling in GC–MS

Analysis of Fatty acid (FA) composition data (Table 3) showed significant variations in the levels of saturated, monounsaturated, and polyunsaturated fatty acids in different trophic mode grown diatom cultures. Eight different fatty acids were identified in the FAME mixture of diatom lipids in phototrophic mode, while fourteen different fatty acids were obtained in hetero and mixotrophic cultures. Fig. 9 highlights the GC peaks obtained at different retention times for different trophic modes. The dominance of C16 – C18 methyl esters contributing up to 91.54% and 90.94% of FAME in hetero- and mixotrophic cultures indicates good quality biodiesel. The dominant fatty acids in the case of autotrophic (PT) culture were palmitoleic (C16:1), palmitic acid (C16:0), with 74.16% of the total fatty acids. Short-chain (C14:0) fatty acid, i.e., myristic acid, ranges up to 11.084% in PT. Higher proportions of saturates such as palmitates and stearates, and oleates signify superior fuel properties with better ignition capabilities owing to higher cetane numbers and better oxidative stability [5,73]. Earlier studies on *Navicula cincta* [74] revealed palmitoleic (53.6%) and palmitic acid (26.5%) at higher levels with superior biodiesel qualities. Low levels of polyunsaturated fatty acids (PUFAs) and saturated fatty acids (SFAs) are commonly recommended for biodiesel exhibiting favorable characteristics, as these FA's, when present at minimal levels, improve oxidative stability and cold flow properties of the fuel [53,73]. SFAs were found to be in major proportion with a total mass percent of 54.21% for PT culture extracted oil, while for heterotrophic (HT) and mixotrophic (MT) cultures, MUFAs exhibited a dominant share with 55.14% and 54.3%, respectively. Earlier investigations have reported that feedstock rich in chain lengths C16 – C18 with SFA and MUFA fatty acids, namely palmitic (C16:0), stearic (C18:0), oleic (C18:1), linoleic (C18:2) and linolenic (C18:3) would produce better quality biodiesel [75]. FAME composition profiles of different green microalga strain *Chlorella* spp. grown under different nutritional modes were reported to dominate by three prominent fatty acid methyl esters, namely palmitic acid (C16:0), Oleic acid (C18:1), and linoleic acid (C18:2), contributing up to 70 – 90% of the FAMEs under all tested treatments [76-78]. In heterotrophic (HT) culture-derived FAME, oleic acid (C18:1) was the dominant fatty acid, followed by palmitic (C16:0) and palmitoleic (C16:1) acid with masses 24.37% and 17.45% out of the total FAs. The percentage of MUFAs, 55.14% out of the total fatty acid composition, was the highest among all nutritional modes. Palmitoleic (C16:1) and Oleic (C18:1) acids were dominant with 28.49% and 25.41%. Minimal levels of long-chain essential fatty acids with carbon lengths of C20 – C24 were observed in both HT and MT-derived oil. Eicosapentaenoic acid (EPA) (C20:5) was present at 1.23%, and lignoceric acid (C24:0) was present at 0.65% in mixotrophic cultivation showing potential applications in

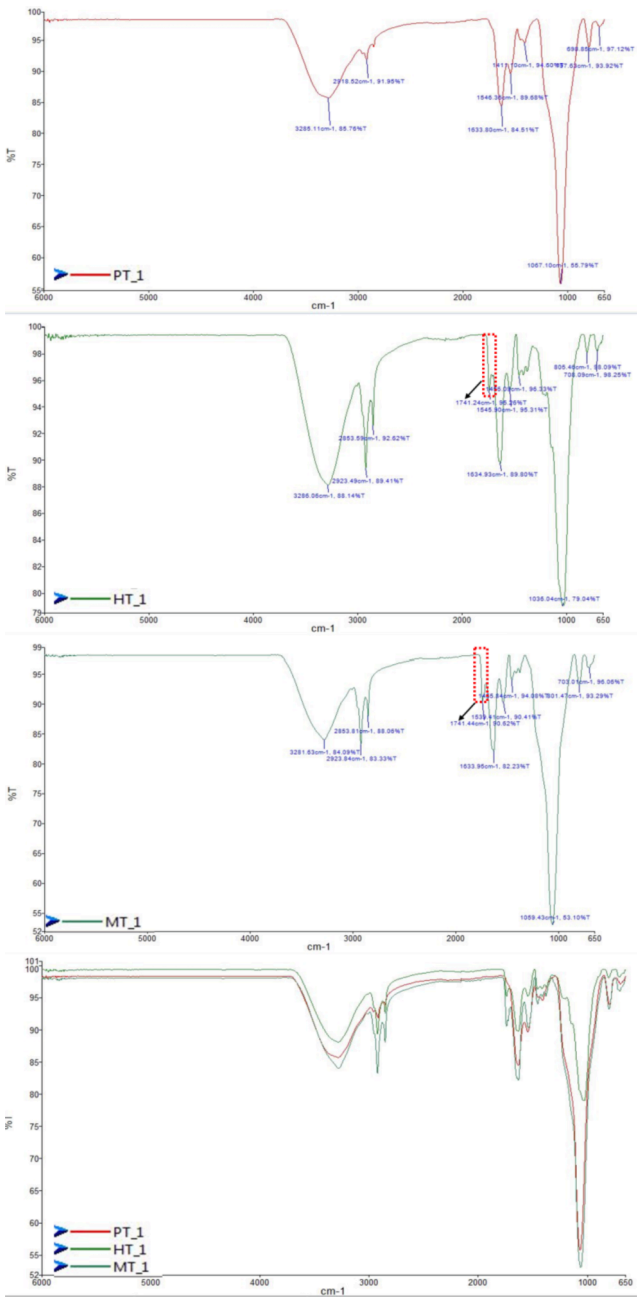

Fig. 7. FT-IR absorption spectra of diatoms under different nutritional modes.

nutraceutical and pharmaceutical industries.

The ω-3 polyunsaturated fatty acids like Eicosapentaenoic acid (EPA) production during mixotrophic cultivation would lead to its promising scope in therapeutic, pharma, and nutraceutical applications. In earlier studies, diatoms grown under mixotrophic conditions produced higher levels of EPA, and EPA was found to increase by two folds in mixotrophically grown cultures of *Phaeodactylum tricornutum* [30]. Diatoms *Navicula saprophila, Nitzschia* sp. were reported to accumulate EPA in levels of ~ 18.5% and 32.0% of the total fatty acids, respectively, when grown at 15 °C [28]. The diatom *Nitzschia laevis* was found to accumulate 2.58% of EPA on a dry cell weight basis of the biomass [79]. Fig. 10 shows the breakup of SFAs, MUFAs, and PUFAs in varying nutritional modes. Thus, optimising process parameters for enhancing the production of ω-3 PUFAs in *Nitzschia* sp. during mixotrophic cultivation might open wide avenues for EPAs as specialty PUFA foods (nutraceuticals) and biofuels.

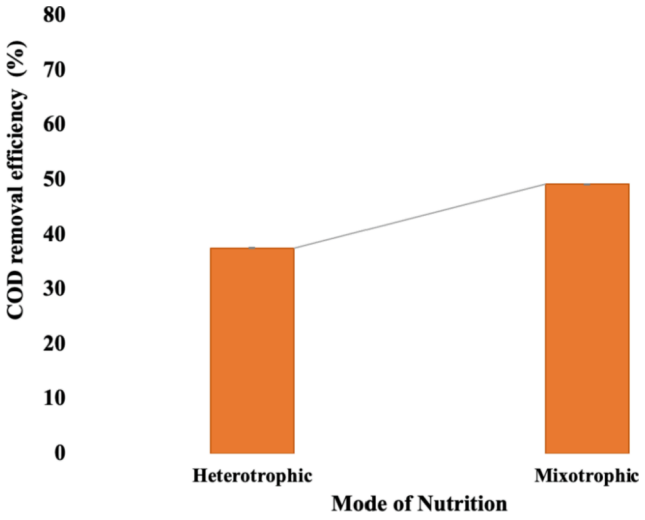

Fig. 8. Percentage of glucose consumed by diatoms during the growth period.

Table 3
FAME composition of lipids extracted from diatoms grown under different trophic modes.

Type of FAME	Lipid No.	% Composition (w/w)		
		PT	HT	MT
Lauric acid, methyl ester	C12:0	–	0.83 ± 0.01	0.78 ± 0.02
Myristic acid, methyl ester	C14:0	4.87 ± 0.87	1.83 ± 0.05	2.62 ± 0.04
n-Pentadecanoic acid, methyl ester	C15:0	11.084 ± 1.76	3.51 ± 0.11	4.20 ± 0.05
Palmitoleic acid, methyl ester	C16:1	41.39 ± 0.70	17.45 ± 1.30	28.49 ± 0.38
Palmitic acid, methyl ester	C16:0	32.77 ± 0.14	24.37 ± 0.32	23.15 ± 0.59
cis-10-Heptadecenoic acid, methyl ester	C17:1n7c	–	3.11 ± 0.10	3.49 ± 0.39
Margaric acid, methyl ester	C17:0	–	1.03 ± 0.19	0.79 ± 0.02
Linoleic acid, methyl ester	C18:2 n6c		3.90 ± 0.19	4.35 ± 0.23
Elaidic acid, methyl ester	C18:1n9t	1.97 ± 0.16	–	–
trans-Vaccenic acid, methyl ester	C18:1n6t	2.97 ± 0.06	–	–
Oleic acid, methyl ester	C18:1n9c		34.58 ± 0.35	25.81 ± 0.68
Stearic acid, methyl ester	C18:0	1.67 ± 0.60	7.10 ± 0.14	4.86 ± 0.12
cis-10-Nonadecenoic acid, methyl ester	C19:0	–	0.61 ± 0.03	0.69 ± 0.03
Eicosanoic acid methyl ester	C20:0	–	0.56 ± 0.09	1.18 ± 0.13
5,8,11,14,17-Eicosapentaenoic acid, methyl ester, (all-Z)-	C20:5	–	0.80 ± 0.13	1.23 ± 0.15
Lignoceric acid methyl ester	C24:0	1.55 ± 0.59	0.65 ± 0.09	1.01 ± 0.09
Squalene	C30:0	2.27 ± 0.43	–	–
Total		100	100	100
C16 – C18		80.77	91.54	90.94
∑(MUFA + PUFA)/∑SFA ratio		0.85	1.47	1.61

3.10. Testing of biodiesel quality

Biodiesel properties can vary substantially for the physical and chemical properties of the feedstock. Generally, direct evaluation of biodiesel properties requires large volumes of biodiesel [54]. However, biodiesel property analysis using predictive models based on fatty acid

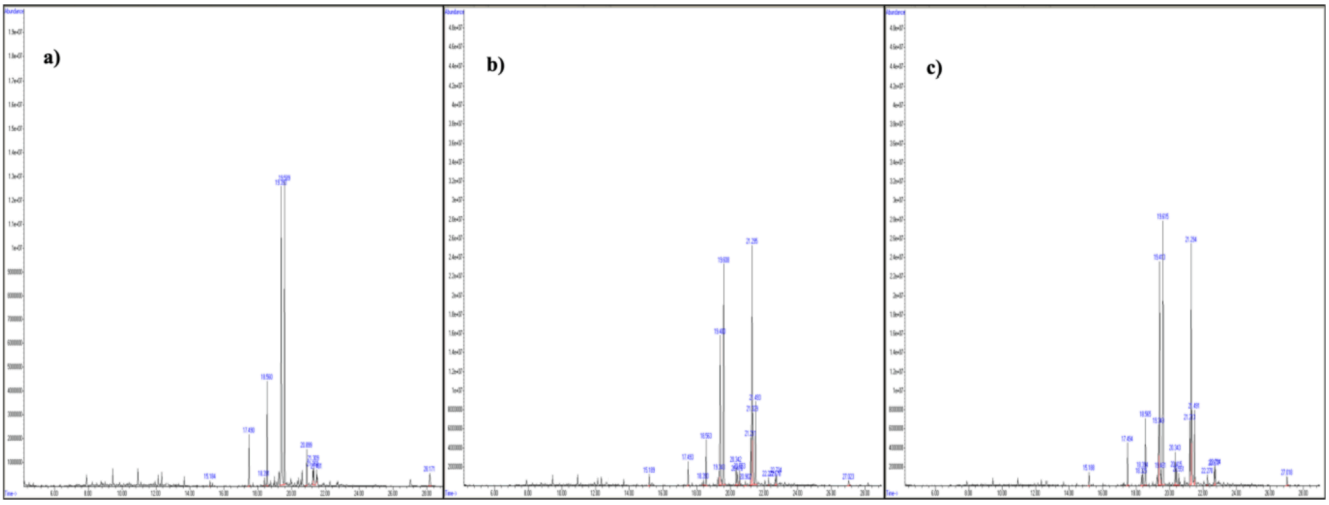

Fig. 9. FAME peaks for varying nutritional mode obtained diatom lipids in GCMS.

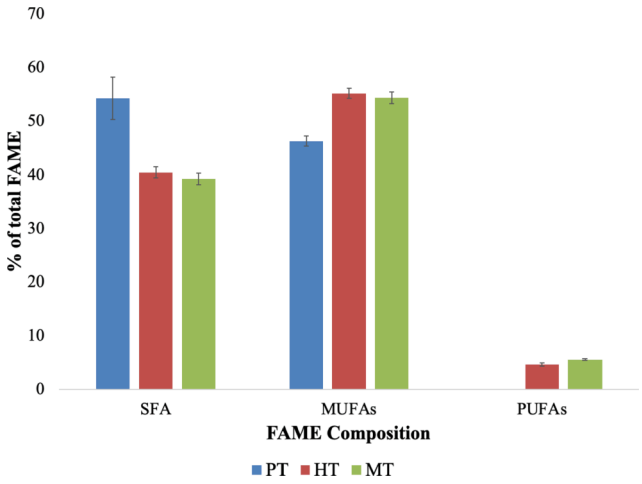

Fig. 10. Percentage of SFAs, MUFAs, and PUFAs in different nutritional modes.

composition is relatively easy, requires much lesser sample volume, and less time-consuming. Many predictive models [53,80,81] have been built so far to predict the properties of biodiesel. Equations of Hoekman [53] were chosen for this study based on its reported closeness to measured values [54]. The biodiesel properties of the oil extracted from all PT, HT, and MT were well within the ASTM specified standard limits. The calculated average degree of unsaturation (ADU) correlates with biodiesel properties, especially cetane number and oxidative stability. Cetane number is the fundamental property of a biofuel that determines the ignition characteristics. The lower the cetane number, means higher is the ignition delay [82]. Generally, higher degrees of unsaturation reduce the cetane (CN) index rating of the fuel, rendering poor oxidative stability and reduce biodiesel quality. The cetane number of diatom-derived biodiesel in this study far exceeds the minimum prescribed requirement of CN: 51 (EN 14214) and CN: 47 (ASTM D975) with 59.8 (PT), 59.1 (HT), and 58.1 (MT). CN ratings of diatoms *Navicula* sp. and *Phaeodactylum tricornutum* [54] reported earlier were lesser than that of the present study with CN 56.7 and CN 55.1, respectively. Cloud point (CP) acts as a decisive parameter in defining a biodiesel's cold flow property. It is only at this temperature the biodiesel starts to form crystals that can clog fuel filters, leading to poor engine performance colder temperatures [83]. CP is defined as the temperature at which the first visible solids start to appear upon cooling the biodiesel. Cold flow properties depend on the quantity and nature of saturated esters over unsaturated ones. The saturates with higher melting point increase cloud point temperatures rendering solidity of the fuel at temperatures below CP, thus hampering its cold flow properties [84]. The cloud point of the biodiesel derived from mixotrophic cultures was found to be the least (10.4 °C), followed by heterotrophic (12.5 °C) and photoautotrophic cultures (13.8 °C), respectively. Standard specification levels of CP are flexible as the parameter is location and season-specific owing to different climatic conditions prevailing around the world [85]. Kinematic viscosity is a critical parameter that ensures adequate fuel reaching the injector at different operating conditions [86]. Kinematic viscosity increases with increasing chain length but decreases with the number of cis carbon double bonds [85]. The limits set by ASTM and EN for kinematic viscosity are 1.9 – 6.0 $mm^2\ S^{-1}$ and 3.5 – 5.0 $mm^2\ S^{-1}$. Irrespective of the nutritional modes, the diatom biodiesel's kinematic viscosity was within the prescribed viscosity range. Kinematic viscosity of diatom-derived biodiesel was 4.9 $mm^2\ S^{-1}$ irrespective of the trophic modes, thus exhibiting concurrence with biodiesel fuel standards. The FAME-derived HHV's of all the treatments were found to comply with standard biodiesel specifications (39.8 – 40.4 MJ kg^{-1}). Iodine value (IV) is a parameter that reflects the degree of unsaturation usually estimated using the unsaturated fatty acid content of the fuel. Iodine value is generally associated with chemical stability of fuel, with lower IV elucidating a higher induction period and improved resistance to oxidation of the fuel [87]. The IV values of *Nitzschia* sp. derived biodiesel (~47 gI_2/100 g oil) in the present study, was well within the EN 14214 standard prescribed levels. The green microalgae *Nannochloropsis oculata* exhibited an IV of 81 gI_2/100 g [86], which is higher than the values obtained in this study. This highlights that the *Nitzschia* sp. derived biodiesel met the biodiesel quality standards with superior biodiesel quality. Table 4 lists the fuel properties tested and their corresponding biodiesel standard specifications.

4. Conclusion

The present investigations focused on variations in growth, morphology, biochemical composition, and fatty acid profiles of the pennate diatom *Nitzschia punctata*. The exploitation of EPS secreted in the form of mucilage stalks exuded by the diatom due to trophic mode variation of *Nitzschia* sp. could be of significant interest in food, pharmaceutical, and nutraceuticals industries. Higher biomass achieved (139.16 ± 3 mg L^{-1}) in mixotrophy shows potential industrial utilisation. From the perspective of biodiesel production using mixotrophically grown diatoms, the results elucidate higher proportions of saturates and MUFAs, especially C16:0, C16:1, and C18:1 up to ~91%, which renders superior quality biodiesel. Moreover, optimizing the process parameters

Table 4
Comparison of biodiesel quality among different nutritional mode extracted oil with ASTM and EN biodiesel standard.

Fuel property	Algal biodiesel			Biodiesel standard	
	PT	HT	MT	ASTM D6751-08	EN 14214
Cetane number	59.8	59.1	58.1	47	51 – 120
HHV (MJ/kg)	39.3	39.5	39.8	–	–
Iodine number (gI_2/100 g)	47.1	54.4	66.4	–	<120
Specific gravity (kg L^{-1})	0.9	0.9	0.9	–	0.86 – 0.90
Density (kg/m^3)	870	870	869	–	860 – 900
Cloud point (°C)	13.8	12.5	10.4	LD*	–
Kinematic viscosity 40 °C (mm^2 S^{-1})	4.9	4.9	4.8	1.9 – 6.0	3.5 – 5.0
Avg. unsaturation	0.46	0.56	0.72	–	–

LD*: Location Dependent.

for enhancing the levels of ω-3 polyunsaturated fatty acids such as Eicosapentaenoic acid (EPA) would open wider avenues for successfully commercialising high-value molecules and associated bioproducts.

Data and accessibility

Data used in the analyses are compiled from the field. Data is anlysed and organized in the form of table, which are presented in the manuscript. Also, synthesized data are archived at http://wgbis.ces.iisc.ernet.in/energy/water/paper/researchpaper2.html#ce and http://wgbis.ces.iisc.ernet.in/biodiversity/.

Authors contribution

Saranya G: Isolation and characterisation, Design and Carrying out experiments, analysis and interpretation of data; and Paper writing.

Ramachandra T V: data analysis and interpretation of data; revising the article critically for important intellectual content; final editing.

Funding

The financial support from ISRO – IISc space technology cell [ISTC/BES/TVR/389] and Gajanana and Madhavi Hegde [CES/TVR/GJH001] endowment fund for biofuel research.

Research ethics

The publication is based on the original research and has not been submitted elsewhere for publication or web hosting.

Animal ethics

The research does not involve either humans, animals or tissues.

Permission to carry out fieldwork

Our research is commissioned by the Ministry of Science and Technology (NRDMS Division), Government of India and hence no further permission is required as the field work was carried out in in the non-restricted areas / protected areas.

Infrastructure support rendered by central facilities of IISc – Society for Innovation and Development for Mass spectroscopy (GC-MS) analysis, Micro Nano characterization Facility (MNCF) CeNSE IISc for SEM EDS imaging and FT-IR analysis, Bioimaging facility under Department of Microbiology and Cell Biology, IISc for confocal microscopy imaging is gratefully acknowledged.

Declaration of Competing Interest

The authors declare that they have no known competing financial interests or personal relationships that could have appeared to influence the work reported in this paper.

Acknowledgments

The authors acknowledge the financial support from ISRO – IISc space technology cell [ISTC/BES/TVR/389] and Gajanana and Madhavi Hegde [CES/TVR/GJH001] endowment fund for biofuel research. Infrastructure support rendered by central facilities of IISc – Society for Innovation and Development for Mass spectroscopy (GC-MS) analysis, Micro Nano Characterisation Facility (MNCF) CeNSE IISc for SEM-EDS imaging and FT-IR analysis, Bioimaging facility under Department of Microbiology and Cell Biology, IISc for confocal microscopy imaging is gratefully acknowledged.

References

[1] Martins F, Felgueiras C, Smitkova M, Caetano N. Analysis of fossil fuel energy consumption and environmental impacts in European countries. Energies 2019;12:1–11. https://doi.org/10.3390/en12060964.
[2] Ramachandra TV, Hegde G. Energy Trajectory in India: Challenges and Opportunities for Innovation. J Resour Energy Dev 2015;12(1-2):1–24. https://doi.org/10.3233/RED-120115.
[3] Wan M, Liu P, Xia J, Rosenberg JN, Oyler GA, Betenbaugh MJ, et al. The effect of mixotrophy on microalgal growth, lipid content, and expression levels of three pathway genes in Chlorella sorokiniana. Appl Microbiol Biotechnol 2011;91(3):835–44. https://doi.org/10.1007/s00253-011-3399-8.
[4] Lang X, Dalai AK, Bakhshi NN, Reaney MJ, Hertz PB. Preparation and characterization of bio-diesels from various bio-oils. Bioresour Technol 2001;80:53–62. https://doi.org/10.1016/S0960-8524(01)00051-7.
[5] Mahapatra DM, Chanakya HN, Ramachandra TV. Euglena sp. as a suitable source of lipids for potential use as biofuel and sustainable wastewater treatment. J Appl Phycol 2013;25(3):855–65. https://doi.org/10.1007/s10811-013-9979-5.
[6] Barnwal BK, Sharma MP. Prospects of biodiesel production from vegetable oils in India. Renew Sustain Energy Rev 2005;9(4):363–78. https://doi.org/10.1016/j.rser.2004.05.007.
[7] Chojnacka K, Facundo-Joaquin, Marquez-Rocha. Kinetic and stoichiometric relationships of the energy and carbon metabolism in the culture of microalgae. Biotechnology (Faisalabad) 2003;3(1):21–34. https://doi.org/10.3923/biotech.2004.21.34.
[8] Chisti Y. Biodiesel from microalgae. Biotechnol Adv 2007;25(3):294–306. https://doi.org/10.1016/j.biotechadv.2007.02.001.
[9] Huang GH, Chen F, Wei D, Zhang XW, Chen G. Biodiesel production by microalgal biotechnology. Appl Energy 2010;87(1):38–46. https://doi.org/10.1016/j.apenergy.2009.06.016.
[10] Chen C-Y, Yeh K-L, Aisyah R, Lee D-J, Chang J-S. Cultivation, photobioreactor design and harvesting of microalgae for biodiesel production: a critical review. Bioresour Technol 2011;102(1):71–81. https://doi.org/10.1016/j.biortech.2010.06.159.
[11] Illman AM, Scragg AH, Shales SW. Increase in Chlorella strains calorific values when grown in low nitrogen medium. Enzyme Microb Technol 2000;27(8):631–5. https://doi.org/10.1016/S0141-0229(00)00266-0.
[12] Mandal S, Mallick N. Microalga Scenedesmus obliquus as a potential source for biodiesel production. Appl Microbiol Biotechnol 2009;84(2):281–91. https://doi.org/10.1007/s00253-009-1935-6.
[13] Yoo C, Jun S-Y, Lee J-Y, Ahn C-Y, Oh H-M. Selection of microalgae for lipid production under high levels carbon dioxide. Bioresour Technol 2010;101(1):S71–4. https://doi.org/10.1016/j.biortech.2009.03.030.
[14] LIU A-Y, CHEN W, ZHENG L-L, SONG L-R. Identification of high-lipid producers for biodiesel production from forty-three green algal isolates in China. Progress in Natural Science: Materials International 2011;21(4):269–76. https://doi.org/10.1016/S1002-0071(12)60057-4.
[15] Lewin JC, Lewin RA. Auxotrophy and heterotrophy in marine littoral diatoms. Can J Microbiol 1960;6(2):127–34. https://doi.org/10.1139/m60-015.
[16] Perez-Garcia O, Bashan Y, Bashan Y, Bashan Y. Microalgal heterotrophic and mixotrophic culturing for bio-refining: From metabolic routes to techno-economics. Algal Biorefineries: Volume 2: Products and Refinery Design 2015:61–131. doi: 10.1007/978-3-319-20200-6_3.
[17] Chen F. High cell density culture of microalgae in heterotrophic growth. Trends Biotechnol 1996;14(11):421–6. https://doi.org/10.1016/0167-7799(96)10060-3.
[18] Cerón Garcí MC, Fernández Sevilla JM, Acién Fernández FG, Molina Grima E, García CF. Mixotrophic growth of Phaeodactylum tricornutum on glycerol: Growth rate and fatty acid profile. J Appl Phycol 2000;12:239–48. https://doi.org/10.1023/A:1008123000002.
[19] Cid A, Abalde J, Herrero C. High yield mixotrophic cultures of the marine microalga Tetraselmis suecica (Kylin) Butcher (Prasinophyceae). J Appl Phycol 1992;4(1):31–7. https://doi.org/10.1007/BF00003958.

[20] Zhang Z, Sun D, Wu T, Li Y, Lee Y, Liu J, et al. The synergistic energy and carbon metabolism under mixotrophic cultivation reveals the coordination between photosynthesis and aerobic respiration in Chlorella zofingiensis. Algal Res 2017; 25:109–16. https://doi.org/10.1016/j.algal.2017.05.007.
[21] Mahapatra DM, Chanakya HN, Ramachandra TV. Bioremediation and lipid synthesis through mixotrophic algal consortia in municipal wastewater. Bioresour Technol 2014;168:142–50. https://doi.org/10.1016/j.biortech.2014.03.130.
[22] Roostaei J, Zhang Y, Gopalakrishnan K, Ochocki AJ. Mixotrophic microalgae biofilm: a novel algae cultivation strategy for improved productivity and cost-efficiency of biofuel feedstock production. Sci Rep 2018;8:12528. https://doi.org/10.1038/s41598-018-31016-1.
[23] Li T, Kirchhoff H, Gargouri M, Feng J, Cousins AB, Pienkos PT, et al. Assessment of photosynthesis regulation in mixotrophically cultured microalga Chlorella sorokiniana. Algal Research 2016;19:30–8. https://doi.org/10.1016/j.algal.2016.07.012.
[24] Chen F, Johns MR. A strategy for high cell density culture of heterotrophic microalgae with inhibitory substrates. J Appl Phycol 1995;7(1):43–6. https://doi.org/10.1007/BF00003548.
[25] Griffiths DJ, Thresher CL, Street HE. The heterotrophic nutrition of Chlorella vulgaris (Brannon No. 1 Strain): with two figures in the text. Ann Bot 1960;24: 1–11. https://doi.org/10.1093/oxfordjournals.aob.a083682.
[26] Stephens E, Ross IL, King Z, Mussgnug JH, Kruse O, Posten C, et al. An Economic and Technical Evaluation of Microalgal Biofuels. n.d.
[27] Perez-Garcia O, Escalante FME, de-Bashan LE, Bashan Y. Heterotrophic cultures of microalgae: metabolism and potential products. Water Res 2011;45(1):11–36. https://doi.org/10.1016/j.watres.2010.08.037.
[28] Kitano M, Matsukawa R, Karube I. Changes in eicosapentaenoic acid content of Navicula saprophila, Rhodomonas salina and Nitzschia sp. under mixotrophic conditions. J Appl Phycol 1997;9:559–63. https://doi.org/10.1023/A:1007908618017.
[29] Lewin J, Hellebust JA. Heterotrophic nutrition of the marine pennate diatom Nitzschia angularis var. affinis. Mar Biol 1976;36(4):313–20. https://doi.org/10.1007/BF00389192.
[30] Ceron Garcia MC, Camacho FG, Mirón AS, Sevilla JMF, Chisti Y, Grima EM. Mixotrophic production of marine microalga Phaeodactylum tricornutum on various carbon sources. J Microbiol Biotechnol 2006;16:689.
[31] Fábregas J, Morales ED, Lamela T, Cabezas B, Otero A. Mixotrophic productivity of the marine diatom Phaeodactylum tricornutum cultured with soluble fractions of rye, wheat and potato. World J Microbiol Biotechnol 1997;13:349–51. https://doi.org/10.1023/A:1018551527986.
[32] Wang H, Fu R, Pei G. A study on lipid production of the mixotrophic microalgae Phaeodactylum tricornutum on various carbon sources. African J Microbiol Res 2012;6:1041–7.
[33] Hellebust JA. Glucose uptake by cyclotella cryptica: dark induction and light inactivation of transport system. J Phycol 1971;7:345–9. https://doi.org/10.1111/j.1529-8817.1971.tb01530.x.
[34] Villanova V, Fortunato AE, Singh D, Bo DD, Conte M, Obata T, et al. Investigating mixotrophic metabolism in the model diatom phaeodactylum tricornutum. Philos Trans Royal Society B: Biol Sci 2017;372(1728):20160404. https://doi.org/10.1098/rstb.2016.0404.
[35] Liu X, Duan S, Li A, Xu N, Cai Z, Hu Z. Effects of organic carbon sources on growth, photosynthesis, and respiration of Phaeodactylum tricornutum. J Appl Phycol 2009;21(2):239–46. https://doi.org/10.1007/s10811-008-9355-z.
[36] Hellebust A. Heterotrophic nutrition of the marine pennate diatom, Cylindrotheca fusiformis. Canadian Journal of Microbiology 1970;16. doi: 10.1139%2Fm70-188.
[37] Wen Z-Y, Chen F. Heterotrophic production of eicosapentaenoid acid by the diatom Nitzschia laevis: effects of silicate and glucose. vol. 25. 2000.
[38] Cooksey KE, Chansang H. Isolation and physiological studies on three isolates of amphora (Bacillariophyceae). J Phycol 1976;12:455–60. https://doi.org/10.1111/j.1529-8817.1976.tb02873.x.
[39] Sheehan J, Dunahay T, Benemann J, Roessler P. Look Back at the U.S. Department of Energy's Aquatic Species Program: Biodiesel from Algae; Close-Out Report. 1998. doi: 10.2172/15003040.
[40] Ramachandra TV, Mahapatra DM, B K, Gordon R. Milking diatoms for sustainable energy: biochemical engineering versus gasoline-secreting diatom solar panels. Ind Eng Chem Res 2009;48(19):8769–88. https://doi.org/10.1021/ie900044j.
[41] Marella TK, Parine NR, Tiwari A. Potential of diatom consortium developed by nutrient enrichment for biodiesel production and simultaneous nutrient removal from waste water. Saudi J Biol Sci 2018;25(4):704–9. https://doi.org/10.1016/j.sjbs.2017.05.011.
[42] Kumar V, Kashyap M, Gautam S, Shukla P, Joshi KB, Vinayak V. Fast Fourier infrared spectroscopy to characterize the biochemical composition in diatoms. J Biosci 2018;43(4):717–29. https://doi.org/10.1007/s12038-018-9792-z.
[43] Saranya G, Subashchandran MD, Mesta P, Ramachandra TV. Prioritization of prospective third-generation biofuel diatom strains. Energy Ecol Environ 2018;3 (6):338–54. https://doi.org/10.1007/s40974-018-0105-z.
[44] Taylor JC, Harding WR, Archibald CGM. A methods manual for the collection, preparation and analysis of diatom samples. 2007. doi: 10.2307/2963468.
[45] Van Heurck H. Van Heurck 1896 - A Treatise on the Diatomaceae. Translated by W. E. Baxter. | Citations - Diatoms of North America 1896. https://diatoms.org/citations/van_heurck_h-1896-a_treatise_on_the_diatomaceae_translated_by_we_baxter (accessed August 18, 2018).
[46] Krammer K and Bertolet H. Krammer, K. Lange-Bertalot, H. (1986) Bacillariophyceae. 1. Teil: Naviculaceae In: Ettl, H., J. Gerloff, H. Heynig and D. Mollenhauer (eds.) Süsswasserflora von Mitteleuropa, Band 2/1. 1986.
[47] Rohit MV, Venkata MS. Quantum yield and fatty acid profile variations with nutritional mode during microalgae cultivation. Front Bioeng Biotechnol 2018;6: 111. https://doi.org/10.3389/fbioe.2018.00111.
[48] Strickland JDH, Parsons TR. A practical handbook of seawater analysis. Bulletin 167. Fisheries Research Board of Canada Bulletin 1972;167:310.
[49] Liu Z-Y, Wang G-C, Zhou B-C. Effect of iron on growth and lipid accumulation in Chlorella vulgaris. Bioresour Technol 2008;99(11):4717–22. https://doi.org/10.1016/j.biortech.2007.09.073.
[50] Satpati GG, Pal R. Rapid detection of neutral lipid in green microalgae by flow cytometry in combination with Nile red staining—an improved technique. Annals of Microbiology 2015;65(2):937–49. https://doi.org/10.1007/s13213-014-0937-5.
[51] Miller GL. Use of dinitrosalicylic acid reagent for determination of reducing sugar. Anal Chem 1959;31(3):426–8. https://doi.org/10.1021/ac60147a030.
[52] Johnson MB, Wen Z. Production of biodiesel fuel from the microalga *Schizochytrium limacinum* by direct transesterification of algal biomass. Energy Fuels 2009;23(10):5179–83. https://doi.org/10.1021/ef900704h.
[53] Hoekman SK, Broch A, Robbins C, Ceniceros E, Natarajan M. Review of biodiesel composition, properties, and specifications. Renew Sustain Energy Rev 2012;16(1): 143–69. https://doi.org/10.1016/j.rser.2011.07.143.
[54] Song M, Pei H, Hu W, Ma G. Evaluation of the potential of 10 microalgal strains for biodiesel production. Bioresour Technol 2013;141:245–51. https://doi.org/10.1016/j.biortech.2013.02.024.
[55] Underwood GJC, Paterson DM. The importance of extracellular carbohydrate productionby marine epipelic diatoms. Adv Botanical Res 2003;40:183–240. https://doi.org/10.1016/S0065-2296(05)40005-1.
[56] Decho AW, Gutierrez T. Microbial extracellular polymeric substances (EPSs) in ocean systems. Front Microbiol 2017;8. https://doi.org/10.3389/fmicb.2017.00922.
[57] Underwood GJC, Boulcott M, Raines CA, Waldron K. Environmental effects on exopolymer production by marine benthic diatoms: dynamics, changes in composition and pathways of production. J Phycol 2004;40:293–304. https://doi.org/10.1111/j.1529-8817.2004.03076.x.
[58] Chiovitti A, Molino P, Crawford SA, Teng R, Spurck T, Wetherbee R. The glucans extracted with warm water from diatoms are mainly derived from intracellular chrysolaminaran and not extracellular polysaccharides. Eur J Phycol 2004;39(2): 117–28. https://doi.org/10.1080/0967026042000201885.
[59] Hufford TL, Collins GB. The stalk of the diatom Cymbella Cistula: Sem observations. J Phycol 1972;8:208–10. https://doi.org/10.1111/j.1529-8817.1972.tb04029.x.
[60] Higgins MJ, Crawford SA, Mulvaney P, Wetherbee R. Characterization of the adhesive mucilages secreted by live diatom cells using Atomic Force Microscopy. Protist 2002;153(1):25–38. https://doi.org/10.1078/1434-4610-00080.
[61] Drum RW. Electron microscope observations of diatoms. Österreichische Botanische Zeitschrift 1969;116(1-5):321–30. https://doi.org/10.1007/BF01379632.
[62] Wustman BA, Gretz MR, Hoagland KD. Extracellular matrix assembly in diatoms (Bacillariophyceae): I. A model of adhesives based on chemical characterization and localization of polysaccharides from the marine diatom Achnanthes longipes and other diatoms. vol. 113. 1997. doi: 10.1104/pp.113.4.1059.
[63] Wustman BA, Lind J, Wetherbee R, Gretz MR. Extracellular matrix assembly in diatoms (Bacillariophyceae): III. Organization of Fucoglucuronogalactans within the adhesive stalks of Achnanthes Iongipes. Plant Physiol 1998;116:1431–41. https://doi.org/10.1104/pp.116.4.1431.
[64] Kuczynska P, Jemiola-Rzeminska M, Strzalka K. Photosynthetic pigments in diatoms. Mar Drugs 2015;13:5847–81. https://doi.org/10.3390/md13095847.
[65] Sánchez-Saavedra MP, Voltolina D. Effect of photon fluence rates of white and blue-green light on growth efficiency and pigment content of three diatom species in batch cultures. Ciencias Marinas 2002;28:273–9. https://doi.org/10.7773/cm.v28i3.225.
[66] Morales-Sánchez D, Tinoco-Valencia R, Kyndt J, Martinez A. Heterotrophic growth of Neochloris oleoabundans using glucose as a carbon source. Biotechnol Biofuels 2013;6(1):100. https://doi.org/10.1186/1754-6834-6-100.
[67] Shen XF, Chu FF, Lam PKS, Zeng RJ. Biosynthesis of high yield fatty acids from Chlorella vulgaris NIES-227 under nitrogen starvation stress during heterotrophic cultivation. Water Res 2015;81:294–300. https://doi.org/10.1016/j.watres.2015.06.003.
[68] Yang C, Hua Q, Shimizu K. Energetics and carbon metabolism during growth of microalgal cells under photoautotrophic, mixotrophic and cyclic light-autotrophic/dark-heterotrophic conditions. Biochem Eng J 2000;6(2):87–102. https://doi.org/10.1016/S1369-703X(00)00080-2.
[69] Bertozzini E, Galluzzi L, Penna A, Magnani M. Application of the standard addition method for the absolute quantification of neutral lipids in microalgae using Nile red. J Microbiol Methods 2011;87(1):17–23. https://doi.org/10.1016/j.mimet.2011.06.018.
[70] Tasic M, Rios P, Santos F, Filipini F, Maciel F. Estimating the elemental biomass composition of Desmodesmus sp. cultivated in sugarcane stillage. vol. 5. 2016. doi: 10.5937/savteh1602033t.
[71] Laurens LML, Wolfrum EJ. Feasibility of spectroscopic characterization of algal lipids: Chemometric correlation of NIR and FTIR Spectra with exogenous lipids in algal biomass. Bioenergy Res 2011;4(1):22–35. https://doi.org/10.1007/s12155-010-9098-y.
[72] Stehfest K, Toepel J, Wilhelm C. The application of micro-FTIR spectroscopy to analyze nutrient stress-related changes in biomass composition of phytoplankton algae. Plant Physiol Biochem 2005;43(7):717–26. https://doi.org/10.1016/j.plaphy.2005.07.001.

[73] Knothe G. Dependence of biodiesel fuel properties on the structure of fatty acid alkyl esters. Fuel Process Technol 2005;86(10):1059–70. https://doi.org/10.1016/j.fuproc.2004.11.002.
[74] Bielsa GB, Popovich CA, Rodríguez MC, Martínez AM, Martín LA, Matulewicz MC, et al. Simultaneous production assessment of triacylglycerols for biodiesel and exopolysaccharides as valuable co-products in Navicula cincta. Algal Research 2016;15:120–8. https://doi.org/10.1016/j.algal.2016.01.013.
[75] Knothe G. Improving biodiesel fuel properties by modifying fatty ester composition. Energy Environ Sci 2009;2:759–66. https://doi.org/10.1039/b903941d.
[76] Gao C, Zhai Y, Ding Yi, Wu Q. Application of sweet sorghum for biodiesel production by heterotrophic microalga Chlorella protothecoides. Appl Energy 2010;87(3):756–61. https://doi.org/10.1016/j.apenergy.2009.09.006.
[77] Zhang K, Sun B, She X, Zhao F, Cao Y, Ren D, et al. Lipid production and composition of fatty acids in Chlorella vulgaris cultured using different methods: Photoautotrophic, heterotrophic, and pure and mixed conditions. Ann Microbiol 2014;64(3):1239–46. https://doi.org/10.1007/s13213-013-0766-y.
[78] Rosenberg JN, Kobayashi N, Barnes A, Noel EA, Betenbaugh MJ, Oyler GA. Comparative analyses of three Chlorella species in response to light and sugar reveal distinctive lipid accumulation patterns in the microalga C. sorokiniana. PLoS ONE 2014;9:e92460. doi: 10.1371/journal.pone.0092460.
[79] Wen Z-Y, Chen F. Continuous cultivation of the diatom Nitzschia laevis for eicosapentaenoic acid production: Physiological study and process optimization. Biotechnol Prog 2002;18(1):21–8. https://doi.org/10.1021/bp010125n.
[80] Nascimento IA, Marques SSI, Cabanelas ITD, Pereira SA, Druzian JI, de Souza CO, et al. Screening microalgae strains for biodiesel production: lipid productivity and estimation of fuel quality based on fatty acids profiles as selective criteria. Bioenergy Res 2013;6(1):1–13. https://doi.org/10.1007/s12155-012-9222-2.
[81] Francisco ÉC, Neves DB, Jacob-Lopes E, Franco TT. Microalgae as feedstock for biodiesel production: carbon dioxide sequestration, lipid production and biofuel quality. J Chem Technol Biotechnol 2010;85(3):395–403. https://doi.org/10.1002/jctb.2338.
[82] Benjumea P, Agudelo J, Agudelo A. Basic properties of palm oil biodiesel-diesel blends 2007. doi:10.1016/j.fuel.2007.11.004.
[83] Dunn RO, Shockley MW, Bagby MO. Improving the low-temperature properties of alternative diesel fuels: vegetable oil-derived methyl esters. JAOCS, J Am Oil Chemists' Society 1996;73(12):1719–28. https://doi.org/10.1007/BF02517978.
[84] Imahara H, Minami E, Saka S. Thermodynamic study on cloud point of biodiesel with its fatty acid composition. Fuel 2006;85(12-13):1666–70. https://doi.org/10.1016/j.fuel.2006.03.003.
[85] Knothe G. A technical evaluation of biodiesel from vegetable oils vs. algae. Will algae-derived biodiesel perform? Green Chem 2011;13:3048–65. https://doi.org/10.1039/c0gc00946f.
[86] Islam MA, Magnusson M, Brown RJ, Ayoko GA, Nabi MN, Heimann K. Microalgal species selection for biodiesel production based on fuel properties derived from fatty acid profiles. Energies 2013;6:5676–702. https://doi.org/10.3390/en6115676.
[87] Sergeeva YE, Mostova EB, Gorin KV, Komova AV, Konova IA, Pojidaev VM, et al. Calculation of Biodiesel Fuel Characteristics Based on the Fatty Acid Composition of the Lipids of Some Biotechnologically Important Microorganisms. Original Russian Text © YaE Sergeeva 2017;53(8):807–13. https://doi.org/10.1134/S0003683817080063.